# Iron Carbide Formation inside Carbon Nanotubes

B.A. Kulnitsky*, V.D. Blank

*Technological Institute of Superhard and New Carbon Materials,
7a, Tsentralnaya St. Troitsk, Moscow, 142190, Russia*

* Corresponding author: Tel. +7 499 400 62 25. *E-mail*: boris@tisnum.ru

**Abstract**

Carbon nanotubes were obtained in conditions of chemical vapor deposition, using iron as a catalyst. Inside the nanotubes, iron carbides belonging to different groups were detected by electron microscopy: prismatic carbides, in which the carbon atoms were in trigonal prismatic interstices, and the octahedral carbide $\zeta$–$Fe_2C$, in which carbon atoms were in octahedral interstices. Information on octahedral iron carbides in the literature is quite limited. Octahedral carbides are difficult to identify, since they are metastable and formed in nano-quantities. It is assumed that plastic deformation can transform the prismatic packing of carbon atoms into octahedral one. In this respect, carbon nanotubes are a unique construction. During the high-temperature growth of nanotubes, the catalytic particle undergoes mechanical compression from the side of the nanotube walls, as a result of which various carbides including the octahedral carbide $\zeta$–$Fe_2C$ can be formed inside the nanotubes.

## Introduction

The discovery of carbon nanotubes [1] aroused great interest in them and led to numerous studies and searches for directions of their possible use. At present, a number of promising directions have been identified, in which carbon nanotubes can be used [2–5]. These include the creation of materials with high mechanical properties, for example, heavy-duty yarns and composite materials, the manufacture of devices for microelectronics, for example, field emitters, supercapacitors, solar cells, etc. Materials for medicine, capsules for gas storage, miniature sensors for analyzing the gaseous medium, etc. are also being developed. Much attention has always been paid to the interaction of carbon nanotubes with different elements that could fill a nanotube. Of interest are tubes, the inner cavity of which is filled with some filler material. Metals and their derivatives, being inside nanotubes, can promote the appearance of unique optical, electronic, mechanical or magnetic properties in nanotubes [6, 7]. Nanotubes can also be of interest as a reaction chamber. These are processes occurring inside nanotubes during their catalytic growth. The catalytic particle, being inside the nanotube, is subjected both to mechanical compression on the side of the walls of the nanotube, and to the chemical action in the atmosphere of gases inside the nanotube. In this case, carbides can be formed and mutually transformed. Such processes can be considered as model in the nano-world and can shed light on the mutual conversions of the phases of the catalyst. In this study, nanotubes were grown by chemical vapor deposition using iron as a catalyst. Interconversion in iron and its derivatives cause a constant interest in metallurgy, since they affect the properties of iron-based alloys. The experimental conditions in this research contributed to the realization of various chemical reactions inside the nanotubes, which in turn led to the formation of a number of iron carbides. In the present study, by the methods of transmission electron microscopy, the phase composition and the defect structure of the catalytic particles inside the carbon nanotubes were studied.

## Experimental

Nanotubes were produced in a continuous stream of CO in a horizontal reactor. The catalyst used was the α-iron powder obtained by decomposition of Fe(CO)$_5$, with a particle size of not more than 3 μm. A ceramic boat with a catalyst was placed in a reactor in an argon atmosphere. The reaction was carried out for 1.5 hours. The maximum temperature in the working area of the reactor was 350–500 °C. A detailed description of the setup is given in [8]. Electron microscopy was carried out on a JEM-2010 instrument equipped with two detachable devices: an energy dispersive spectrometer (**EDS**) that allows analyzing the characteristic X-ray emission spectra and the electron energy loss spectrometer (**EELS**). Samples were prepared using a standard procedure: the obtained powder was applied to a copper mesh previously coated with a special carbonaceous base coat.

## Results and discussion

According to electron microscopic analysis, multi-walled carbon nanotubes, most of them containing segmented cavities, were observed in the sample. Nanotubes did not always have the right shape. This is due to the non-equilibrium conditions in the synthesis process. Inside the nanotubes, iron-containing compounds, mainly various iron carbides, were found. In addition to carbides, nanotubes often contained iron in pure form: both the α- and γ-phases, which were approximately in a ratio of 1 : 1. Sometimes particles with a crystal lattice corresponding to the γ-phase were twinned. It is believed that during the decomposition of Fe(CO)$_5$, iron is formed, which can be considered as a starting material during the growth of nanotubes [7]. Thus, in the part of nanotubes, α → γ transformation occurred in iron.

Fig. 1 shows photographs of the α- and γ- particles of iron formed inside the nanotubes during the synthesis. Under normal conditions, the α-phase of iron, which has a body-centered crystal lattice (**BCL**) with a parameter $a = 0.287$ nm, is stable. At a temperature of 916 °C [9], the γ-phase is formed, which has a face-centered crystal lattice (**FCL**) with a parameter of 0.365 nm. When pressure is applied, the temperature of this transformation decreases. In addition, it is known that for particles of small size, the parameters of certain processes vary. In [10], arguments are presented in favor of the fact that the γ-phase of iron can also be formed inside the nanotube as a result of growth, in the same way as in a miniature high-pressure chamber. The presence of a γ-particle of iron in a nanotube at room temperature is surprising, but this was observed in [11, 12] and was explained by the fact that, while inside the nanotube, the γ-particle of iron cannot transform in the α-iron particle after expansion because of high mechanical properties of the graphene shell. Some studies describe experiments in which ferrocene as a precursor for chemical vapor deposition was used, and both iron phases were simultaneously detected inside the nanotubes [13]. Carbon nanotubes containing α- and γ-iron particles were synthesized also in [14] by the pyrolysis method. In the present work, it was not possible to fix particles in which the α- and γ-phases of iron were simultaneously present.

Fig. 2 shows a fragment of a nanotube with a cementite particle (θ−Fe$_3$C). The inset shows the Fourier transform of image $a$. Fig. 2 $b$ shows an enlarged image of the fragment indicated by the square in Fig. 2 $a$.

Fig. 3 shows fragments of carbides Fe$_5$C$_2$ ($a$) and Fe$_7$C$_3$ ($b$) found in nanotubes in this study. The formation of carbides inside nanotubes growing with the use of iron as a catalyst includes several
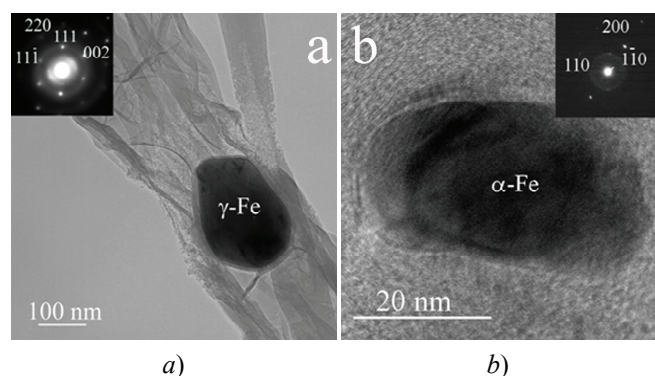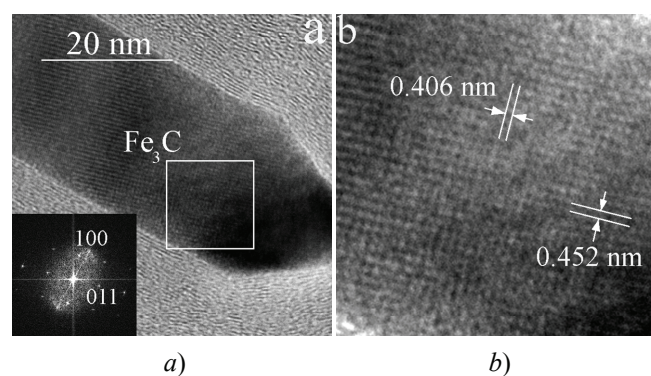


*a)*          *b)*

**Fig. 1. Fragments of nanotubes with γ-article of iron (*a*) and α-particle of iron. The insets show the corresponding microdiffraction patterns (*b*)**



*a)*          *b)*

**Fig. 2. Fragment of a nanotube with a cementite particle (Fe$_3$C):**
*a* – image and its Fourier transform (in the inset);
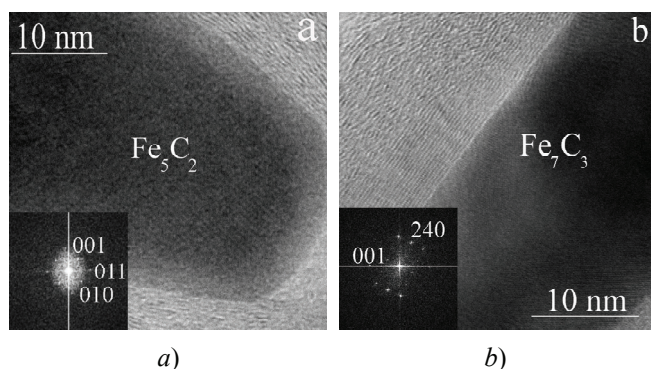*b* – an enlarged image of the fragment indicated by a square in *a*

**Fig. 3. Two iron carbides:**
$Fe_5C_2$ (*a*) and $Fe_7C_3$ (*b*) found in nanotubes.
The inset shows the Fourier transform of the image

processes, primarily the diffusion of carbon, both bulk and surface. Such diffusion can occur even at room temperature. Carbon atoms penetrating into the metal particle are distributed regularly in interstices and then they move in the process of diffusion in various directions, accumulating in different places and forming different types of defects. The displacement of carbon atoms in the material leads to distortions of the crystal lattice. The carbon atoms cluster and form local clusters. Such clusters grow and form embryos of carbides [15].

Today, a large number of iron carbides the composition of which varies from FeC to $Fe_4C$ are known. The most known is cementite, a chemical compound in iron-carbon alloys. The chemical formula of cementite is $Fe_3C$ and the carbon concentration is 6.67 % (by weight). The crystal lattice of cementite is orthorhombic with the parameters: $a = 0.452$ nm, $b = 0.509$ nm and c = 0.674 nm. It is believed that the transformation of iron into cementite occurs through ε-carbide. For the first time such transformation path was proposed in [16]. In this case, the planes $(11–22)_ε$ and $(001)_{Fe3C}$ are parallel. There are two options for this transformation:

$$(11–22)_ε \text{ II } (001)_{Fe3C} \text{ II } (211)_α \text{ and}$$

$$(11–22)_ε \text{ II } (001)_{Fe3C} \text{ II } (21-5)_α.$$

Both these orientational relations (**OR**) were detected experimentally [7]. Hegg's carbide $χ–Fe_5C_2$ [17] with a monoclinic crystal lattice and with the parameters $a = 1.156$ nm, $b = 0.456$ nm $c = 0.503$ nm and $β = 98.3°$ is less common. There are three carbides of $Fe_7C_3$ composition, different in crystal lattices. Thus, the lattice of hexagonal carbide has the following parameters: $a = 0.688$ nm, $C = 0.454$ nm; orthorhombic carbide has the following parameters: $a = 0.6879$ nm, $b = 1.1942$ nm, c = 0.454 nm; pseudo-hexagonal carbide has the following parameters: $a = 1.3982$ nm and $c = 0.4506$ nm.

It is known that iron carbides, depending on the position of carbon atoms in the iron sublattice, can be divided into octahedral, tetrahedral and trigonal-prismatic. [18]. Fig. 4 shows the arrangement of the carbon atom among the iron atoms in octahedral and prismatic carbides. The most stable is $θ–Fe_3C$ carbide with a trigonal-prismatic structure centered by a carbon atom (Fig. 2 *a*). This carbide is found most often in iron-carbon steels. There is also known $ε–Fe_3C$ cementite, in which the carbon atom is located in the octahedral pore in the iron sublattice. In other words, carbon atoms can be found in cementite, both in prismatic and octahedral pores in the iron sublattice. Polyhedra of the six iron atoms surrounding the carbon atom are also characteristic for the structures of $Fe_5C_2$ and $Fe_7C_3$ carbides (Fig. 3 *a*, *b*). Carbon nanofibers with iron carbide particles with the highest concentration of carbon ($Fe_7C_3$) were produced in a gas-static unit at a nitrogen pressure of about 70 MPa [8]. Hyde [19] described the idea of a polysynthetic twin model, from which it follows that $Fe_7C_3$ carbide can easily be obtained from $θ–Fe_3C$ carbide. The prismatic model is also characteristic of the crystal lattice of Hagg's carbide ($Fe_5C_2$). This carbide can be formed in a wide range of temperatures. It is known that catalytic particles of $Fe_5C_2$ were found in carbon nanotubes and nanofibers grown by chemical vapor deposition under pyrolysis conditions of polyethylene in the temperature range from 500 to 1000 °C [20]. Carbides $Fe_5C_2$ and $Fe_3C$ can be converted into each other, which was confirmed in [20, 21], in which both $Fe_5C_2$ layers in $Fe_3C$ and vice versa were found. It was shown in [20] that Hagg's carbide was destroyed under the short-term action of an electron beam by an explosive method with conversion to $Fe_3C$ or to γ-Fe. It follows that the formation of the γ-phase of iron inside the nanotubes found in this study can be explained not only by the result of the pressure
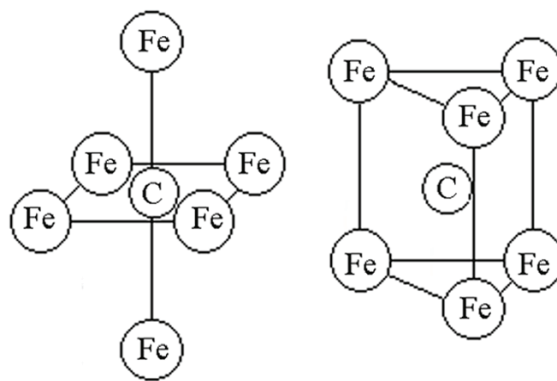


**Fig. 4. Arrangements of carbon atoms among the iron atoms in octahedral and prismatic carbides**

inside the nanotube, but also by the result of the following reaction: $\alpha$-Fe $\rightarrow$ Fe$_5$C$_2\rightarrow$ $\gamma$-Fe.

Fe$_7$C$_3$ carbide can exist in three different crystalline structures: hexagonal, orthorhombic and pseudo-hexagonal [21]. Fig. 2 *c* shows a particle with a pseudo-hexagonal lattice, although other variants of the Fe$_7$C$_3$ structure were observed in the present study. The formation of trigonal prismatic iron carbides in carbon structures (nanotubes, nanofibres) was observed repeatedly [22–25].

Fig. 5 shows photographs of iron carbide, the identification of which caused difficulties. The crystal lattice did not correspond to any of the above carbides. The analysis showed that the most suitable was the crystal lattice, corresponding to the $\zeta$-carbide of iron. Fig. 5 *a*, b shows fragments of nanotubes with $\zeta$–Fe$_2$C carbide. Fig. 5 *a* shows a fragment of the $\zeta$-carbide of iron; the Fourier transform of the image is shown in the inset; Fig. 5 *b* shows an enlarged image of the fragment shown in Fig. 5 *a* in the square. It is believed that at pressures of the inner core of the earth (330–364 GPa) carbides of composition Fe$_2$C are the most stable [26]. The data described in [27], indicate the existence of iron carbides of Fe$_2$C composition, other than the known carbide with a hexagonal structure. Thus, by analogy with Co$_2$N and Fe$_2$N, the existence of carbide was suggested. This carbide is described by an orthorhombic lattice with the parameters: $a = 0.429$ nm, $b = 0.546$ nm and $c = 0.448$ nm, and has a hexagonal close-packed iron sublattice. In [28], it was noted that within the orthorhombic lattice, variants of the cementite structure with different arrangement of iron and carbon atoms with respect to each other could arise. Therefore, cementite will depend on the initial heat treatment in two or more structural states. Trigonal prismatic carbides are described in many articles, whereas information on octahedral carbides is

quite limited. Octahedral carbides are difficult to identify, since they are metastable and formed in nano-quantities. It is interesting to note that two iron carbides of composition Fe$_2$C ($\zeta$- and $\eta$-) have close crystal lattices and are described by the Pnnm (58) and Pbcn (60) spatial groups, respectively.) In our case, the analysis confirms that Fig. 5 *a* shows $\zeta$-carbide. Fig. 6 shows another nanotube containing the same carbide. The inset shows the Fourier transform of the image. The arrows indicate fragments of the particle corresponding to Fourier transforms of the image. In the left part, the structure corresponds to $\zeta$-carbide, and in the right part, it indicates polytypism along the plane (010).

Calculations from the first principles show that the prismatic cell has the lowest energy, and that the energy difference between the octahedral and prismatic modifications is less than the characteristic energy of plastic deformation during mechanical fusion. Thus, plastic deformation can strongly affect the structure. It is known that octahedral carbides are formed by a martensitic route at 250 °C. At low temperatures, octahedral carbides transform into trigonal prismatic carbides. Octahedral carbides of composition Fe$_2$C and Fe$_{2.2}$C are converted to $\chi$-Fe$_5$C$_2$ at a higher temperature than 250 °C and further in $\theta$-Fe$_3$C at a temperature exceeding 350 °C. The exact temperature of the transformation depends on many factors such as crystal size, morphology, surface texture, etc. [29].

Currently, experimental data on cementite indicate that the positions of carbon atoms depend on the conditions of mechanical and thermal treatments [30, 31]. The lattice in which the carbon is in prismatic positions is the ground state in full accordance with the experimental results. Plastic deformation can transform the prismatic packing of carbon atoms into octahedral. The difference in the energies of the two
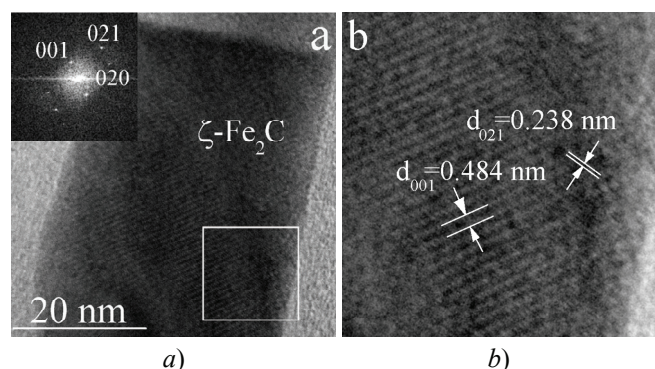


*a)*                                  *b)*

**Fig. 5. $\zeta$-iron carbide:**
*a* – fragment of $\zeta$-iron carbide; the inset shows
the Fourier transform of the image; *b* – an enlarged image
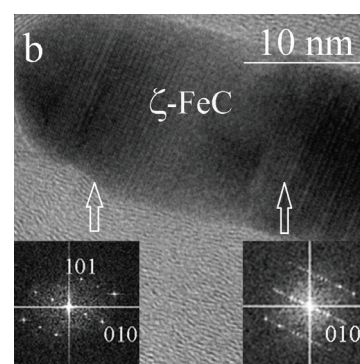of the fragment shown in Fig. *a* in the square



**Fig. 6. $\zeta$-iron carbide. Inserts show the Fourier transform.
The arrows indicate fragments of the particle
corresponding to Fourier transforms**

configurations of the positions of the carbon atoms suggests that, on the one hand, the deformation energy during machining is sufficient to change the positions of the carbon atoms, while, on the other hand, the probability of such displacements of carbon atoms in the process of thermodynamic fluctuations is not high at a temperature not exceeding 700 K. Thus, it can be assumed that both the formation of octahedral carbide ($\zeta$-$Fe_2C$) and the formation of packaging defects that lead to polytypism are the result of deformation at high temperature. The process of catalytic growth of nanotubes involves the dissolution of carbon in a quasi-liquid catalytic particle, the diffusion of carbon in a particle, and its release on the surface of a particle in the form of graphene layers in the case of supersaturation. The interaction of the selected graphene layers and particles leads to a change in the shape of the particle. In [32] it was shown that surface tension forces are involved in this interaction. A catalytic particle can be considered as consisting of atoms of two different elements. In such a crystal, an orientational ordering of atoms occurs in the stress field, which leads to deformation of the crystal. The composition of the crystal determines the maximum deformation. Such deformation is determined by the motion of point defects. In the conditions of nanotube growth, defect migration occurs due to thermal fluctuations, which depend on the process temperature. Since the component of the surface tension force is directed toward the center of the tube at each point of its surface [33], it is clear that the largest amount of pressure will be on the central part of the tube. The formation of nanotubes and the shaping of catalytic particles take place at high temperatures, when the surface tension of the metal is much less than that at a room temperature. Therefore, during cooling, additional deformation of the particle is possible. The described processes explain the defectiveness of particles (twinning, packing defects, polytypism), as well as phase transformations and the simultaneous existence of several phases in the particle. In [34] cementite was produced in the process of metal sputtering from carbon-saturated iron at temperatures not exceeding 650 °C. Hagg's carbide particles inside carbon nanospheres were obtained in [35] at temperatures of 400–600 °C. Cementite is considered as an intermediate phase in metallic sputtering. Thus, Hagg's carbide was formed on the surface of cementite, and then they both disintegrated during sputtering [36]. Both these carbides were also formed in carburizing experiments in the $CO$–$H_2$–$H_2O$–$H_2S$ atmosphere. The Gibbs energy $\Delta G$ for the formation of $Fe_5C_2$ was found to be equal to 500 °C. This result agrees with other literary data. Thus, at a temperature in the region of 350 °C, the equilibrium of three phases: $\alpha$-$Fe$, $Fe_3C$ and $Fe_5C_2$ is observed [37]. From the perspective of thermodynamics, the great variety of carbides obtained in the present work is not surprising. All carbides are produced during the growth of nanotubes in the same temperature range.

## Conclusion

Carbon nanotubes were produced under the conditions of the vapor deposition method using iron as a catalyst. Inside the nanotubes, the iron and iron phases of BCL- and FCL-phases of iron and iron carbides were found; along with the prismatic trigonal carbides $Fe_3C$, $Fe_5C_2$ and $Fe_7C_3$, the octahedral carbide $\zeta$-$Fe_2C$ were observed.

## Acknowledgement

## References

1. Iijima S., Single-shell carbon nanotubes of 1-nm diameter. *Nature*, 1991, Vol. 354, pp. 56-58.

2. Charlier J.-C., Blase X., Electronic and transport properties of nanotubes. *Review of modern physics*, 2007, Vol.79, pp. 677-732.

3. Ebbesen T.W., Carbon nanotubes. *Physics today*, 1996, Vol. 6, pp. 26-32.

4. Rakov E.G., The chemistry and application of carbon nanotubes. *Russian Chemical Reviews*, 2001, Vol. 70, Issue 10, pp. 827-863.

5. Kiang C.-H., Endo M., Ajayan P.M., Dresselhaus G., and Dresselhaus M.S., Size Effects in Carbon Nanotubes. *Phys. Rev. Lett.*, 1998, Vol. 81, pp.1869-1872.

6. Eletskii A.V., Transport properties of carbon nanotubes, *Physics-Uspekhi*, 2009, Vol. 52, Issue 3, pp. 209-224.

7. Blank V.D., Kulnitskiy B.A., Perezhogin I.A., TEM studies of carbon nanostructures, grown on iron catalyst. Crystallography of iron carbides. In *Carbon nanotubes and related structures*. Eds: Blank V., Kulnitskiy B., 2008, Research Signpost, Trivandrum-695, Kerala, India, pp. 150.

8. Blank V.D., Kulnitskiy B.A., Batov D.V., Bangert U., Gutierrez-Sosa A., Harvey A.J., Electron microscopy and electron energy loss spectroscopy studies of carbon fiber formation at a Fe catalysts. *Journal of Applied Physics*, 2002, Vol. 91, Issue 3, pp. 1657-1660.

9. Tonkov E.Yu., Ponyatovsky E.G., *Phase transformations of elements under high pressure*. 2004, CRC Press, pp. 392.

10. Blank, V.D.; Kulnitskiy, B.A.; Perezhogin, I.A.; Alshevsky, Yu.L.; Batov, D.V.; Kazennov, N.V., Nanotube as reaction cell. Deformation processes in nanotubes, *Materialovedenie*, 2007, Vol. 118, Issue 1, 2007, pp. 42-48.

11. Golberg D., Mitome M., Muller Ch., Tang C., Leonhardt A., Bando Y., Atomic structures of iron-based single crystalline nanowires crystallized inside multi-walled carbon nanotubes as revealed by analytical electron microscopy. *Acta Materialia*, 2006, Vol. 54, pp. 2567-2576.

12. Kim H., Sigmund W. Effect of a graphite structure on the stability of fcc iron. *J. of Crystal. Growth*, 2004, Vol. 267, pp. 738-744.

13. Muhl T., Elefant D., Graff A., Kozhuharova R., Leonhardt A., Monch I., Ritschel M., Simon P., Groudeva-Zotova S., Schneider C.M., Magnetic properties of aligned Fe-filled carbon nanotubes. *Journal of Applied Physics*, 2003, Vol. 93, Issue 10, pp. 7894-7896.

14. Prados C., Crespo P., Gonzalez J.M., Hernando A., Marco J.F., Gancedo R., Grobert N., Terrones M., Walton R.M., Kroto H.W., *Phys. Rev. B*, 2002, Vol. 65, pp. 113405-113409.

15. Durand-Charre M., *Microstructure of steels and cast iron*, Springer, 2013, 403 pp.

16. Jack K.H., Structural transformations in the tempering of high-carbon martensiticsteels. *J. Iron Steel. Inst.*, 1951, Vol. 169, pp. 26-36.

17. Duggin M.J., Hofer L.J.E., Nature of χ-Iron Carbide. *Nature*, 1966, Vol. 212, pp. 248-250.

18. Liu X.-W., Zhao S., Meng Y., Peng Q., Dearden A.K., Huo C.-F., Yang Y., Li Y.-W., Wen X.-D., Mossbauer Spectroscopy of iron carbides: from prediction to experimental confirmation. *Scientific reports*, 2016, Vol. 6, pp. 1-10.

19. Hyde B.G., Andersson S., Bakker M., Plug C.M., O'Keeffe M., The (twin) composition plane as an extended defect and structure-building entity in crystals. *Prog. Solid State Chem.*, 1974, Vol. 12, pp. 272-327.

20. Blank V., Kulnitskiy B., Perezhogin I., Alshevskiy Yu., Kazennov N., Decomposition of $Fe_5C_2$ catalyst particles in carbon nanofibers during TEM observation. *Sci. Technol. Adv. Mater.*, 2009, Vol. 10, 015004, pp. 1-5.

21. Audier M., Bowen P., Jones W., Transmission Electron Microscopic Study of Single crystals of Fe7C3. *J. of Crystal Growth*, 1983, Vol. 63, pp. 125-134.

22. Blank V.D., Alshevskiy Yu.L., Zaitsev A.I., Kazennov N.V., Perezhogin I.A., Kulnitskiy B.A., Structure and phase composition of a catalyst for carbon nanofiber formation. *Scripta Materialia*, 2006, Vol. 55, pp. 1035-1038.

23. Blank V.D., Buranova Y.S., Kulnitskiy B.A., Perezhogin I.A., Bagramov R.H., Dubitsky G.A., Formation and crystallographic relations of iron phases and iron carbides inside the carbon nanotubes. *High Temperatures-High Pressures*, 2014, Vol. 43, pp. 39-45.

24. Oberlin A., Endo M., Koyama T., Filamentous growth of carbon through benzene decomposition. *J. Cryst. Growth*, 1976, Vol. 32, Issue 3, pp. 335-349.

25. Ruston W.R., Warzee M., Hennaut J., Waty J., The solid reaction products of the catalytic decomposition of carbon monoxide on iron at 550 °C. *Carbon*, 1969, Vol. 7, pp. 47-57.

26. Bazhanova Z.G., Oganov A.R., Gianola O., Fe–C and Fe–H systems at pressures of the Earth's inner core. *Physics-Uspekhi*, 2012, Vol. 182, Issue 5, pp. 521-530.

27. Hirotsu Y., Nagakura S., Crystal structure and morphology of the carbide precipitated from martensituc high carbon steel during the first stage of tempering. *Acta Metallurgica*, 1972, Vol. 20, pp. 645-655.

28. Schastlivtsev V.M., Yakovleva I.L., Mirzaev D.A., Okishev K.Y. On the possible positions of carbon atoms in the cementite lattice. *Physics of Metals and Metallography*, 2003, Vol. 96, Issue 3, pp. 75-82.

29. de Smit E., Cinquini F., Beale A.M., Safonova O.V., van Beek W., Sautet P., Weckhuysen B.M., Stability and reaction of ε→χ→θ iron carbide catalyst phases in Fischer-Tropsch synthesis: Controlling $\mu_c$. *J. Am. Chem. Soc.*, 2010, Vol. 132, pp.14928-14941.

30. Arzhnikov A.K., Dobysheva L.V., Demangeat C., Structural peculiarities of cementite and their influence on magnetic characteristics. *J. Phys.: Condens. Matter*, 2007, Vol. 19, pp. 196214 1-9.

31. Audier M., Bowen P., Jones W., Electron microscopic and Mössbauer study of the iron carbides $Fe_3C$ and $Fe_5C_2$ formed during the disproportionation of CO. *J. Crystal Growth*, 1983, Vol. 64, pp. 291-296.

32. Boehm H.P., Carbon from carbon monoxide disproportionation on nickel and iron catalysts: Morphological studies and possible growth mechanisms, *Carbon*, 1973, Vol. 11, no. 6, pp. 583-586.

33. Amelinckx S., *The direct observation of dislocations*. Academic Press, New York, 1964, 487 p.

34. Pippel, E., Woltersdorf, J., Grabke, H.J., Strauss S., Microscopy of mivroprocesses of metal dusting of iron, *Steel. Res.*, 1995, Vol. 5, Issue 66, pp. 217-221.

35. Prilutskiy O., Katz E.A., Shames A.I., Mogilevsky D., Mogilko E., Prilutskiy E., Dub S.N., Synthesis of carbon nanomaterials by a catalytic disproportionation of carbon Monoxide. *Fullerenes, nanotubes and carbon nanostructures*, 2005, Vol.13, Issue 1, pp. 453-456.

36. Schneider A., Grabke H.J., Effect of $H_2S$ on Metal Dusting of Iron. *Mater. Corros.*, 2003, Vol. 54, pp. 793-798.

37. Schneider A., Inden G., Thermodynamics of Hägg carbide ($Fe_5C_2$) formation. *Steel Research*, 2001, Vol. 72, Issue 11-12, pp. 503-507.